AERODYNAMIC PROPERTIES AND OPTIMAL RELEASE CONDITIONS OF TURBO-JAVS

Haruki Nakayama[1], Tomoya Nakajima[2], Tomoaki Itano[1] and Masako Sugihara-Seki[1*]

(Received August 29, 2023; accepted January 16, 2024)

Abstract:

The aerodynamic characteristics of turbo-javs were measured by wind tunnel experiments, and the obtained data were used to compute trajectories of a turbo-jav starting from the initial conditions of 35 throwing experiments. Comparisons between the computed results and the throwing experiments suggested a potential modification for the trajectory computation, such as adding a resistance term to the pitching moment estimated from the wind tunnel experiments. Utilizing this method, we investigated the optimal release conditions for turbo-javs to achieve the maximum flight distance.

1 Introduction

The turbo-jav is used in the javelic throw, which is an official event at the Junior Olympic Games, contested for flight distance similar to the javelin throw. Composed of polyethylene, except for the tip, the turbo-jav distinguishes itself with four wings at the tail (Fig. 1(a)). Comparing the flight of a turbo-jav with wings cut off with that of a turbo-jav with intact wings revealed that the presence of wings stabilizes the turbo-jav's flight, accompanied by an oscillatory pitching motion around the angle of attack ≈ 0[1)]. The aerodynamic forces acting on the turbo-jav play a major role in its flight, and there is considerable interest in identifying the initial conditions under which the maximum possible flight distance can be achieved.

In this study, we conducted (1) wind tunnel experiments, (2) throwing experiments, (3) trajectory computations, and (4) the search for optimal release conditions for the turbo-jav. The wind tunnel experiments focused on investigating the aerodynamic characteristics of turbo-javs, measuring the drag, lift, and pitching moment around the center of mass. Throwing experiments involved capturing images of the release and trajectories of turbo-javs thrown by participants using two cameras. From the initial conditions of each throwing experiment, we computed the trajectory of the center of mass and the variation of the attitude angle of the turbo-jav based on aerodynamic coefficients obtained in the wind tunnel experiments. We assessed how well these computations replicated the throwing experiments. The comparison revealed consistency between the computed results and corresponding throwing experiments when the trajectory computation was modified by adding a resistance

1 Department of Pure and Applied Physics, Kansai University, Suita, Osaka 564-8680, Japan
2 Department of Mechanical Engineering, Osaka Metropolitan University, Sakai, Osaka 599-8531, Japan
* Correspondence to: Masako Sugihara-Seki, Department of Pure and Applied Physics, Kansai University, Suita, Osaka 564-8680. E-mail: sekim@kansai-u.ac.jp

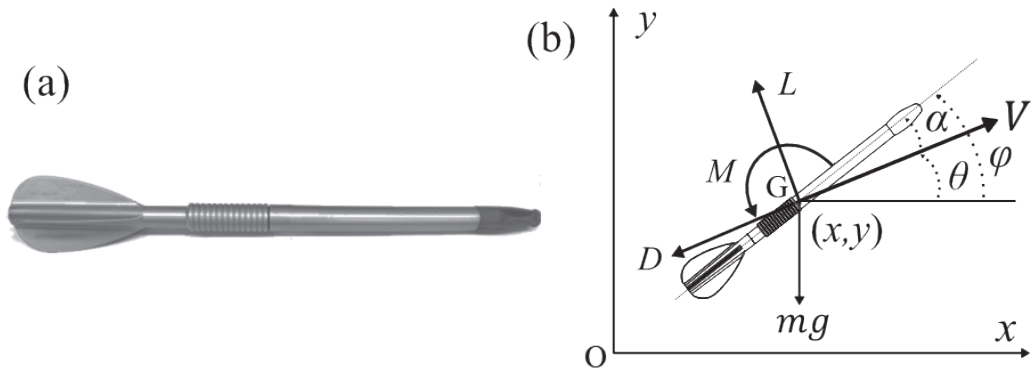

Fig. 1. (a) Photograph of a turbo-jav, and (b) configuration during turbo-jav flights (V: velocity, α: angle of attack, φ: attitude angle, D: drag, L: lift, M: pitching moment). (x,y) represents the center of mass position.

term proportional to the square of the rotational velocity in the pitching moment. Using this new method, we investigated the optimum release conditions for obtaining the maximum flight distance of the turbo-jav.

2 Methods

2.1 Wind tunnel experiments

The wind tunnel experiments were conducted in a Göttingen-type low-speed wind tunnel located at the Department of Mechanical Engineering, Osaka Metropolitan University, Japan. The wind tunnel boasts a maximum wind speed of approximately 25 m/s and a test section of 1.0 m × 1.5 m in cross-section and 3.0 m length. A commercially available turbo-jav (Nishi Sports, Japan) was supported at the center of mass, and the drag force D, lift force L, and pitching moment M were measured using 3-component load cells (LMC-3501A, LMC-3520A, Nissho Denki, Japan). Wind speeds ranged from 12 to 24 m/s, and the turbo-jav's angle of attack was changed every 5° from 0 to 50° relative to the wind direction.

The Reynolds number is defined as $Re=\rho Ul/\mu$, where ρ, μ, U, and l represent the density, viscosity of the air, wind speed, and length of the turbo-jav, respectively (Table 1). In each experiment, the density and viscosity of the air were determined based on the measured temperature. The non-dimensional aerodynamic coefficients, including the drag coefficient, lift coefficient, and moment coefficient, were then calculated as

$$C_d = \frac{D}{\rho U^2 S/2}, \qquad C_l = \frac{L}{\rho U^2 S/2}, \qquad C_m = \frac{M}{\rho U^2 S l/2}, \tag{1}$$

where S denotes the cross-sectional area of the turbo-jav (Table 1).

Table 1 Data of turbo-javs

length l [m]	mass m [kg]	diameter d [m]	cross-sectional area S [m^2]	center of mass position (distance from the tip)[m]	moment of inertia I [kg m^2]
6.96×10^{-1}	3.07×10^{-1}	3.72×10^{-2}	1.09×10^{-3}	3.76×10^{-1}	1.34×10^{-2}

2.2 Throwing experiments

Images of a turbo-jav released by throwers were taken using two cameras. The first camera, a Photron FASTCAM Mini UX50, recorded high-resolution images from immediately before to immediately after the release at a distance of approximately 8 m from the throwers to obtain precise information on the initial conditions. The second camera, a Panasonic LUMIX DC-GH5, recorded the entire trajectory of the released turbo-javs until they landed. In the coordinate system, Fig. 1(b), the origin was set on the ground, with the x-axis in the horizontal direction and the y-axis in the vertical upward direction. A guideline along the x-axis was drawn on the ground, and 35 throws in which the flight was along this guideline with a misalignment angle of less than 1° were regarded as two-dimensional flights in the xy-plane and selected for later analysis. In addition, the length of the turbo-jav in each image was checked to ensure that it lay on the xy-plane. The two cameras were carefully adjusted so that their optical axes were perpendicular to the xy-plane.

From each image recorded, the center of mass (x,y) and attitude angle φ of the released turbo-jav were obtained by automatic analysis using the image recognition library OpenCV. As initial conditions, we carefully detected the release speed V_0, release angle θ_0, initial attitude angle φ_0, initial angular velocity $\dot{\varphi}_0$, and release height y_0. We set $x(0) \equiv x_0=0$, for simplicity.

2.3 Trajectory computations

For the two-dimensional flight of a turbo-jav in the xy-plane, the equations of motion for the center of mass and the pitching motion are expressed in terms of the variables shown in Fig. 1(b) as

$$\begin{cases} m\dfrac{d^2x}{dt^2} = -L\sin\theta - D\cos\theta, & (2) \\ m\dfrac{d^2y}{dt^2} = L\cos\theta - D\sin\theta - mg, & (3) \\ I\dfrac{d^2\varphi}{dt^2} = M, & (4) \end{cases}$$

where m and I represent the mass and moment of inertia about the axis lying at the center of mass, perpendicular to the main axis of the turbo-jav. We only consider cases where the yawing motion can be neglected (see Section 2.2). In this case, the rolling motion can also be neglected in the trajectory analysis, as the full 3-D equations of motion of a turbo-jav indicate that the rolling motion does not affect the pitching motion. From the initial conditions detected in each throwing experiment, equations (2)-(4) are integrated to obtain the temporal evolutions of x, y, and φ. Here, the values of D, L, and M are given in terms of the speed of the turbo-jav V and the aerodynamic coefficients C_d, C_l and C_m as

$$D = \frac{1}{2}C_d\rho V^2 S, \qquad L = \frac{1}{2}C_l\rho V^2 S, \qquad M = \frac{1}{2}C_m\rho V^2 Sl, \tag{5}$$

where C_d, C_l, and C_m are obtained as functions of the angle of attack α from the wind tunnel experiments. Note that in the wind tunnel experiments, the values of D, L, and M were measured at constant angles of attack α, whereas α varies with time during the flight of a turbo-jav. At each moment, the angle θ is calculated as $\theta=\arctan(V_y/V_x)$, where V_x and V_y

represent the x- and y-component of the velocity of the center of mass, and $V = \sqrt{{V_x}^2 + {V_y}^2}$. The angle of attack is calculated as $\alpha = \varphi - \theta$.

2 Results and Discussion

3.1 Experimental and computational results

The aerodynamic coefficients (C_d, C_l, and C_m) obtained at various angles of attack α are plotted as a function of the Reynolds number in Fig. 2(a), showing averaged values and standard deviations from four wind tunnel experiments. The values averaged over the Reynolds number at each angle of attack α are plotted in Fig. 2(b). For $0 \leq \alpha \leq 50°$, C_d increases monotonically with α, while C_l and C_m attain maximum absolute values near $\alpha = 40°$. The negative values of C_m explain the oscillatory pitching motion during the turbo-jav flight[1].

From symmetry considerations, C_d is an even function of α, while C_l and C_m are odd functions. Using this property, we computed the temporal evolutions of (x,y) and α based on equations (2)-(4), starting from the initial conditions of each throwing experiment (simulation A). An example of the trajectory of the center of mass (x,y) and the variation of α with x is plotted in Figs. 3(a),(b), together with the experimental results. Figure 3(a) illustrates that the trajectory of the turbo-jav obtained by simulation A has a lower maximum height and a smaller flight distance than the corresponding values of the throwing experiment. In addition,

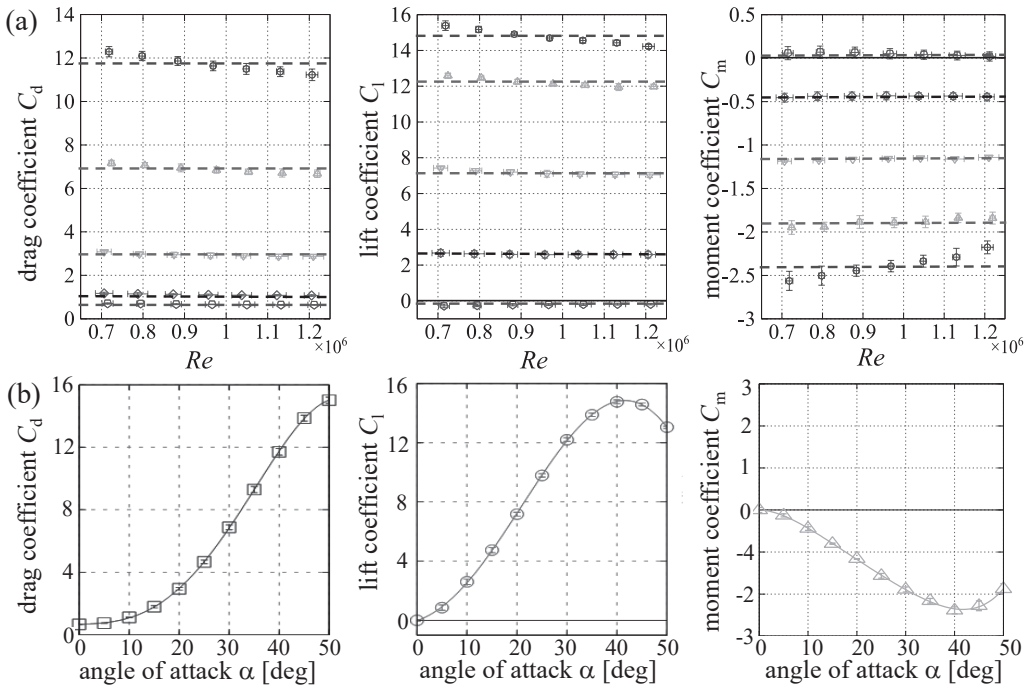

Fig. 2. Results of wind tunnel experiments. (a) Aerodynamic coefficients (C_d, C_l, C_m) vs. Re at $\alpha = 0°$ (pentagon), 10° (diamond), 20° (inverted triangle), 30° (triangle), and 40° (square), and (b) aerodynamic coefficients vs. angle of attack α. In (a), horizontal lines indicate mean values averaged over the Reynolds number. In (b), solid lines represent approximate curves through the data points (mean values at corresponding angles of attack) obtained by cubic spline interpolation.

Fig. 3(b) indicates that the angle of attack obtained by simulation A has a larger amplitude of oscillation compared to the experimental result, suggesting that this property may lead to a lower maximum height and a smaller flight distance of simulation A. These features were commonly observed for the results of simulation A. Thus, we propose adding a resistance term to the pitching moment, which is proportional to the square of the pitching velocity, so that equation (4) is modified as

$$I\frac{d^2\varphi}{dt^2} = \frac{1}{2}C_m\rho V^2 Sl - \frac{1}{2}k\,\mathrm{sign}(\dot{\varphi})\,\rho l^3 S'\dot{\varphi}^2, \tag{6}$$

where k is a non-dimensional parameter, $S' = dl$ (d:diameter of the turbo-jav, Table 1), and $\mathrm{sign}(\dot{\varphi})=1$ (for $\dot{\varphi}>0$) or -1 (for $\dot{\varphi}<0$). Since $l\dot{\varphi}$ represents a measure of the rotational velocity of the pitching motion, the added term in equation (6) (the second term on the right-hand side) is proportional to the square of the rotational velocity of the turbo-jav. In other words, this term results mainly from the oscillatory pitching motion of the turbo-jav during flight.

For various values of k, we integrated equations (2), (3), and (6) (instead of (4)) from the initial conditions detected in each throwing experiment to obtain the temporal evolutions of x, y, and φ (simulation B). Examining 35 throwing experiments, the least square difference between the computed results and the throwing experiments was achieved when adopting k=0.9. The difference in flight distance between measured and simulation B results was within 5 percent in almost all cases. For the case shown in Fig. 3, the results obtained by simulation B using k=0.9 were also plotted in Fig. 3. Figure 3 presents a better match of simulation B results to the experimental results for both the trajectory of the center of mass and the variation of the angle of attack.

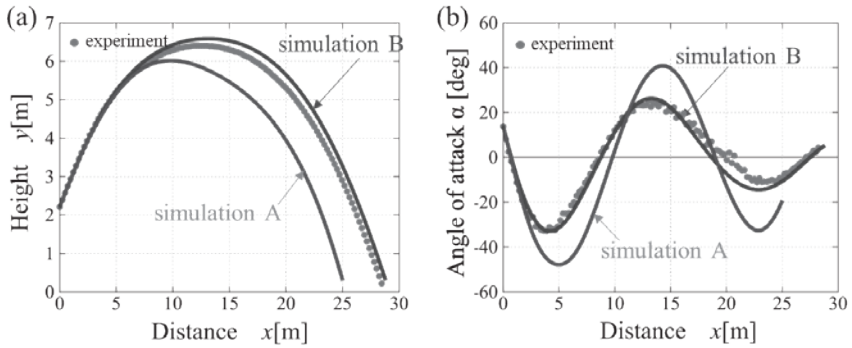

Fig. 3. (a) Trajectories of the center of mass (x,y), and (b) variations of angle of attack α with x (experiments, simulation A & B). The initial conditions are V_0=14.4 m/s, θ_0 ($\equiv \varphi_0 - \alpha_0$)=37.2°, α_0=13.8°, $\dot{\varphi}_0$=−5.35 rad/s, and y_0=2.21m. In simulation B, k is set to be 0.9.

3.2 Search for optimal release conditions

Using equations (2), (3), and (6) with k=0.9, we searched for the optical release conditions (release speed V_0, release angle θ_0, initial attitude angle φ_0, initial angular velocity $\dot{\varphi}_0$, and release height y_0) of turbo-javs to achieve the maximum flight distance. It is evident that the larger V_0, the longer the flight distance[2]. Similarly, a larger y_0 results in a longer flight distance. Thus, the optimal release conditions were investigated for given values of V_0 and y_0. In the case of V_0=16.0 m/s and y_0=2.0 m, the results are shown in Fig. 4 at θ_0=30, 40, and 50°. The numbers in Fig. 4 denote the flight distance. It can be observed in Fig. 4 that α_0 ($\equiv$

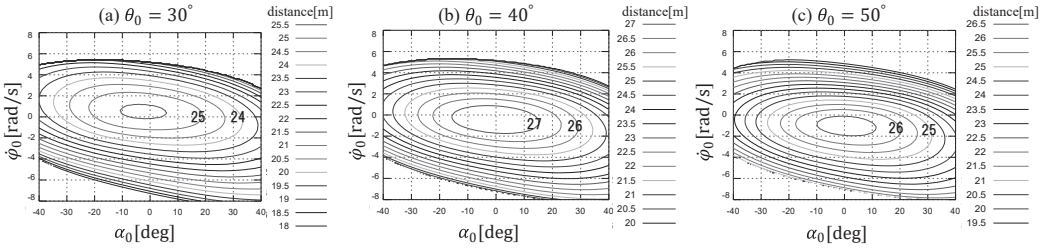

Fig. 4. Relationship between the initial conditions (initial angle of attack α_0, initial angular velocity $\dot{\varphi}_0$) and the flight distance for the release speed V_0=16.0 m/s and release height y_0=2.0 m, obtained by simulation B with k=0.9.

$\varphi_0-\theta_0) \approx 0$ and $\dot{\varphi}_0 \approx 0$ result in the longest flight distance at each release angle θ_0. This tendency may be explained by the fact that the drag is the smallest at the angle of attack $\alpha = 0$ (Fig. 2). Investigations for various values of θ_0 indicated that the optimal release conditions would be θ_0=42~43°, α_0=−3~1°, and $\dot{\varphi}_0$=−0.5~−0.1 rad/s in the case of V_0=12~20 m/s and y_0=2.0 m. Among these optimal initial conditions, negative values of $\dot{\varphi}_0$ may help to keep the angle of attack small, since the slope of the tangent line to the trajectory gradually decreases after the release. In general, the optimal conditions vary depending on the values of V_0 and y_0. However, release conditions of θ_0 smaller than 45°, α_0 close to 0, and $\dot{\varphi}_0$ slightly smaller than 0 would be nearly optimal for obtaining the longest flight, regardless of the values of V_0 and y_0.

4 Conclusions

From the wind tunnel experiments, throwing experiments, and trajectory computations of turbo-javs, we proposed a novel method to calculate the trajectory of the center of mass and the temporal evolution of the attitude angle such that the results are consistent with the results of throwing experiments. Employing this approach, we computed turbo-jav trajectories from various initial conditions and identified the optimal release conditions that led to the maximum flight distance. The optimal conditions were determined to be a release angle smaller than 45°, an initial angle of attack close to 0, and an initial angular velocity of the pitching motion slightly smaller than 0.

References

1) M. Nagao, T. Nakajima, T. Itano and M. Sugihara-Seki. Experimental studies on aerodynamic characteristics of the turbo-jav. *J. JSME B*, **79**, 1561-1570 (2013).

2) M. Maeda and Y. Tanmatsu. Effects of turbo-jav release conditions on throwing distance in javelic throw. *J. Method. Sports*, **21**, 139-145 (2008).